A frequency-domain-based master stability function for synchronization in nonlinear periodic oscillators

A Frequency-domain based Master Stability Function for synchronization in nonlinear periodic oscillators

Marco Righero, Fernando Corinto and Mario Biey
Electronics Dept., Politecnico di Torino, Corso Duca degli Abruzzi 24, I-10129, Torino, Italy
Email:{marco.righero, fernando.corinto, mario.biey}@polito.it

Abstract

An efficient methodology to study conditions for stable in-phase synchronization in networks of periodic identical nonlinear oscillators is proposed. The problem of investigating synchronization properties on periodic trajectories is reduced to an eigenvalue problem by means of the joint application of Master Stability Function and Harmonic Balance techniques. The proposed method permits to exploit the periodicity of trajectories, reducing computational time with respect to traditional time-domain approaches (which were designed to deal with generic attractors) and good accuracy. In addition, such method can easily deal with networks of nonlinear periodic oscillators described by differential-algebraic equations and then both static and dynamic coupling could be studied.

Index Terms

Synchronization, Nonlinear oscillators, Harmonic Balance, Stability.

I. Introduction

The synchronized state in networks of coupled dynamical systems (cells) —namely the phenomenon that occurs when coupled systems adjust their different trajectories to a unison one due to the mutual interactions— is a deeply studied subject [1]–[3]. Beyond rising researchers curiosity per se and the amazing fact that many real world systems exhibit it [1], synchronization is believed to play an important role in information processing in biological neural networks [4], [5], for instance as a way to filter noise [6].

The existence of (locally) stable synchronous states is generally investigated by computing the spectrum of Lyapunov Exponents (LEs) [7] of the whole network. Unfortunately, even when dealing with networks composed of a small number of cells, the size of the problem requires long CPU time and may show numerical instabilities [8]–[10].

In 1998, Pecora and Caroll [11] proposed a technique, subject to some constraints, to simplify this task. The problem of identifying conditions for stable synchronization was split in two parts: one related to network topology and the other requesting the computation of LEs of a system of the same order as a *single* uncoupled oscillator. This second step involves the evaluation of the so called Master Stability Function (MSF) [11]. Notwithstanding a great simplification, as in this case we have to deal with one nonlinear oscillator at a time, the computational effort remains important: for each value of the MSF, one has to identify an attractor and the algorithm estimating the LEs has to reach convergence. The attractor is usually obtained by means of time-domain methods, discarding transient behavior. Moreover, the choice of initial conditions may have an important impact.

In order to take advantage of the periodicity of attractors, spectral methods —for instance Harmonic Balance (HB)— can be employed for identifying an accurate approximation of steady-state periodic oscillations in nonlinear oscillators [12].

The main aim of this manuscript is then to present an efficient method, based on the joint use of HB and MSF techniques, in order to evaluate synchronization properties in networks composed of coupled identical nonlinear oscillators, focusing on *periodic* behavior [13]. Beyond the reduction in CPU time, the HB-based method makes it possible to investigate nonlinear oscillators described by Differential Algebraic Equations (DAEs) [14].

The manuscript is organized as follows. In Section II, we briefly recap the main ideas of HB and how to study stability of periodic state in the frequency domain. In Section III we show how to combine the stability analysis in the frequency domain with the MSF. In Section IV we present some examples to highlight the reduction in CPU time and the accuracy of the resulting algorithm. In particular, we study some cases which are new in literature, to the best of our knowledge, as they could not be investigated with the classic time-domain version of the MSF. Some conclusions are drawn at the end of the paper.

II. Harmonic balance and stability of periodic solutions

For the sake of completeness and to introduce the proper notation, this Section is devoted to briefly summarize how HB technique can be used for:

a) finding cycles;
b) analyzing their stability.

In general, we consider systems whose dynamic is described by [14]–[16]

$$\frac{\mathrm{d}}{\mathrm{d}\,t}[q(x)] + g(x) = 0, \tag{1}$$

with the state variable $x(t) \in \mathbb{R}^L$, and suppose they admit at least a T-periodic solution, which we denote by $x^T(t)$.

Point (a)— We recall that any scalar function $\psi^T(t)$ which is T-periodic can be approximated with the truncated Fourier series

$$\psi(t) \simeq a_0 + \sum_{k=1}^{K} \big(a_k \cos(k\omega t) + b_k \sin(k\omega t)\big), \tag{2}$$

where a_0, a_k, and b_k are the Fourier coefficients and $\omega = 2\pi/T$. Using $M = 2K + 1$ equally spaced time samples $x(t_m)$ in $(0, T]$, with $t_m = mT/M$, $m = 1, \ldots, M$, we can link the Fourier coefficients and the time samples $\psi(t_m)$ using an appropriate matrix Γ with inverse

$$\Gamma^{-1} = \begin{pmatrix} 1 & \gamma^{\mathrm{C}}_{1,1} & \gamma^{\mathrm{S}}_{1,1} & \cdots & \gamma^{\mathrm{C}}_{1,K} & \gamma^{\mathrm{S}}_{1,K} \\ \vdots & \vdots & \vdots & & \vdots & \vdots \\ 1 & \gamma^{\mathrm{C}}_{M,1} & \gamma^{\mathrm{S}}_{M,1} & \cdots & \gamma^{\mathrm{C}}_{M,K} & \gamma^{\mathrm{S}}_{M,K} \end{pmatrix} \in \mathbb{R}^{M\times M}, \tag{3}$$

whose entries are given by

$$\gamma^{\mathrm{C}}_{p,q} = \cos\left(\frac{q2\pi p}{2K+1}\right),\ \gamma^{\mathrm{S}}_{p,q} = \sin\left(\frac{q2\pi p}{2K+1}\right). \tag{4}$$

We have then

$$\Psi^F = \Gamma\Psi,$$

where

$$\Psi = \begin{pmatrix} \psi(t_1) \\ \vdots \\ \vdots \\ \vdots \\ \psi(t_M) \end{pmatrix}, \quad \Psi^F = \begin{pmatrix} a_0 \\ a_1 \\ b_1 \\ \vdots \\ a_K \\ b_K \end{pmatrix}.$$

We can link the Fourier coefficients of the time derivative $\dot{\psi}(t)$, gathered in the column vector $\dot{\Psi}^F$, to the ones of $\psi(t)$ as

$$\dot{\Psi}^F = \omega\Omega\Psi^F, \tag{5}$$

where Ω is a $M \times M$ matrix whose only nonzero entries are $\Omega_{2k,2k+1} = k$ and $\Omega_{2k+1,2k} = -k$, for $k = 1, \ldots, K$. Defining the direct product $\otimes$ between matrices $A \in \mathbb{R}^{N_1 \times M_1}$ and $B \in \mathbb{R}^{N_2 \times M_2}$as

$$A \otimes B = \begin{bmatrix} A_{11}B & A_{12}B & \cdots & A_{1M_1}B \\ A_{21}B & A_{22}B & \cdots & A_{2M_1}B \\ \vdots & \vdots & \ddots & \vdots \\ A_{N_11}B & A_{N2}B & \cdots & A_{N_1M_1}B \end{bmatrix} \in \mathbb{R}^{N_1N_2 \times M_1M_2} \tag{6}$$

and denoting with $\Gamma_L = 1_L \otimes \Gamma$, we have that the vector of the Fourier coefficient X^F of the T-periodic L-dimensional solution $x^T(t)$ is linked to the time samples

$$X = [x_1(t_1) \cdots x_1(t_M)\, x_2(t_1) \cdots x_2(t_M) \cdots x_L(t_1) \cdots x_L(t_M)]',$$

where the apex $'$ denotes transposition, via $X^F = \Gamma_L X$. As described in [17], [18], this formalism can be used to look for the Fourier coefficients of limit cycles for a system $\dot{x} = f(x)$ (setting $g(x) = -f(x)$ and $q(x) = x$) or, more generally, of the form of (1) [14].

Point (b)— We recall that, given a L-dimensional system [14]–[16]

$$\frac{\mathrm{d}}{\mathrm{d}\,t}[C(t)\delta(t)] - A(t)\delta(t) = 0, \tag{7}$$

with $C(t)$ and $A(t)$ T-periodic $L \times L$ matrices, the corresponding L Floquet Multipliers (FMs) $\lambda_\ell = \mathrm{e}^{\mu_\ell T}$ are such that $u_\ell(t)\,\mathrm{e}^{\mu_\ell t}$ are L linearly independent solutions of (7), with $u_\ell(t)$ T-periodic. The Floquet (or characteristic) Exponents (FEs) are the values μ_ℓ and their real part coincide with the LEs [7]. If $C(t)$ and $A(t)$ in (7) are the Jacobian matrices of the vector fields $q(\cdot)$ and $-g(\cdot)$ of (1) evaluated on a periodic solution (a cycle), then the FMs carry information about the local stability of that cycle.

Following [14], we can express the FMs in the HB setting as an eigenvalue problem: $\mathrm{e}^{\mu_\ell T}$ is a FM corresponding to the solution $u_\ell(t)$ (whose time samples form U_ℓ and whose truncated Fourier coefficients form U_ℓ^F, such that $U^F = \Gamma_L U$) if μ_ℓ and U_ℓ are solution to the following generalized eigenvalue problem

$$\left(\Gamma_L A_M \Gamma_L^{-1} - \omega \Omega_M \Gamma_L C_M \Gamma_L^{-1}\right) U_\ell^F = \mu_\ell \Gamma_L C_M \Gamma_L^{-1} U_\ell^F, \tag{8}$$

where A_M and C_M are $LM \times LM$ block matrices constructed expanding each element of A and C in a diagonal block of time samples $A(t_1), \ldots A(t_M)$ and $C(t_1), \ldots C(t_M)$ respectively,

$$A_M = \begin{pmatrix} A_{11}(t_1) & & 0 & & A_{1D}(t_1) & & 0 \\ & \ddots & & \cdots & & \ddots & \\ 0 & & A_{11}(t_M) & & 0 & & A_{1D}(t_M) \\ & \vdots & & \ddots & & \vdots & \\ A_{1D}(t_1) & & 0 & & A_{DD}(t_1) & & 0 \\ & \ddots & & \cdots & & \ddots & \\ 0 & & A_{1D}(t_M) & & 0 & & A_{DD}(t_M) \end{pmatrix}, \tag{9}$$

and $\Omega_L = 1_L \otimes \Omega$. The solutions of (8) gives LM different eigenvalues. These correspond to a subset of the infinitely many FEs μ_ℓ, which determine L independent FM $\mathrm{e}^{\mu_\ell T}$. These eigenvalues are distributed along L vertical lines in the complex plane (see Figure 1 for an example where C is the identity matrix, $L = 3$ and $K = 5$). As noted in [14], to get precise results, we should look for the FEs with smaller imaginary part.

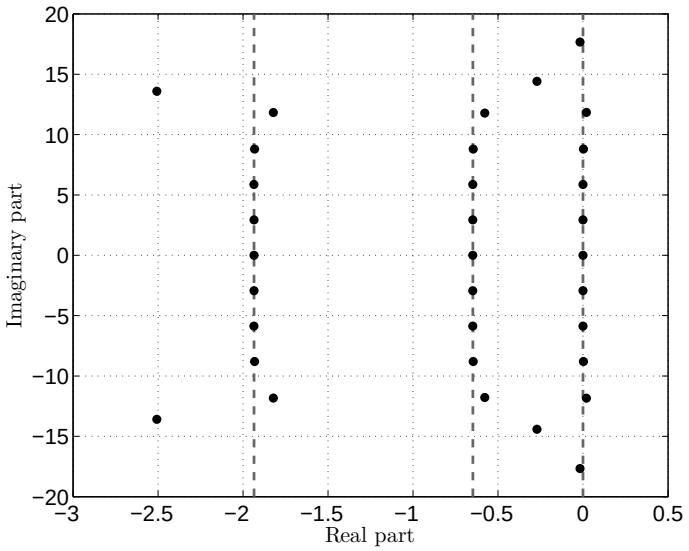

Figure 1. Location on the Gauss plane of the eigenvalues of the systems (8) for a Chua's oscillator ($L = 3$) approximated with $K = 5$.

III. The Master Stability Function in the frequency domain

The MSF permits to study synchronization conditions for networks of coupled nonlinear systems [11]. We summarize the main ideas to point out how spectral methods can be successfully used to conceive efficient algorithms for evaluating synchronization on limit cycles.

We consider networks of N cells described by the model ($n = 1, \dots, N$)

$$\frac{\mathrm{d}}{\mathrm{d}\,t}\left[q(x_n) + v\sum_{n'=1}^{N} Z_{nn'} r(x_{n'})\right] + g(x_n) + w\sum_{n'=1}^{N} Z_{nn'} h(x_{n'}) = 0, \tag{10}$$

where $x_n \in \mathbb{R}^L$ is the L-dimensional state of the n^{th} cell, $q : \mathbb{R}^L \to \mathbb{R}^L$ and $g : \mathbb{R}^L \to \mathbb{R}^L$ account for the nonlinear dynamics of the uncoupled cell, $Z \in \mathbb{R}^{N\times N}$ is the positive semidefinite and with zero row sum matrix describing the coupling among cells, $v, w \in \mathbb{R}$ are overall coupling strengths, and $h : \mathbb{R}^L \to \mathbb{R}^L$ and $r : \mathbb{R}^L \to \mathbb{R}^L$ describe the nonlinear interactions among the cells.

Through the paper, we call *dynamic* and *static* the couplings described by matrices $V = vZ$ and $W = wZ$, respectively.

We are interested in studying conditions on the network topology described by Z in (10) so that the synchronous manifold $x_1 = x_2 = \dots x_n = \dots x_N$ is stable [1]. It is worth noting that the synchronous manifold corresponds to the in-phase periodic oscillation, i.e. there are zero phase shifts among all oscillators.

Denoting by x^T the common T-periodic dynamics on the synchronous manifold —which coincides with the solution of the isolated oscillator described in (1), as the matrix Z has zero row sum— we consider the variational equations associated to (10)

$$\frac{\mathrm{d}}{\mathrm{d}\,t}\left[q(x^T + \delta_n) + v\sum_{n'=1}^{N} Z_{nn'} r(x^T + \delta_{n'})\right] + g(x^T + \delta_n) + w\sum_{n'=1}^{N} Z_{nn'} h(x^T + \delta_{n'}) = 0, \tag{11}$$

where δ_n is an infinitesimal perturbation, with respect to the synchronous solution x^T, of the n-th

[1]Under suitable assumptions on function $f(\cdot)$, stable synchronous manifolds result to be $\rho_1 x_1 = \rho_2 x_2 = \dots = \rho_n x_n = \dots = \rho_N x_N$, where $\rho_n \in \{-1, 1\}$. The results given in this manuscript can be generalized to such stable synchronous manifolds.

cell. Taking the first order expansions of q, g and h and neglecting second-order terms, we get

$$\frac{\mathrm{d}}{\mathrm{d}\,t}\Big[q(x^T) + Dq(x^T)\delta_n + v\sum_{n'=1}^{N} Z_{nn'}\Big(r(x^T) + Dr(x^T)\delta_{n'}\Big)\Big] + \\ + g(x^T) + Dg(x^T)\delta_n + w\sum_{n'=1}^{N} Z_{nn'}\Big(h(x^T) + Dh(x^T)\delta_{n'}\Big) = 0, \quad (12)$$

where $Dq(x^T)$, $Dr(x^T)$, $Dg(x^T)$ and $Dh(x^T)$ are the Jacobian matrices of q, r, g and h, respectively, evaluated on the solution x^T. As $x^T(t)$ is the solution of (1), we have that (12) simplifies to the following

$$\frac{\mathrm{d}}{\mathrm{d}\,t}\Big[Dq(x^T)\delta_n + v\sum_{n'=1}^{N} Z_{nn'}Dr(x^T)\delta_{n'}\Big] + Dg(x^T)\delta_n + w\sum_{n'=1}^{N} Z_{nn'}Dh(x^T)\delta_{n'} = 0, \quad (13)$$

We have now a system of equations of the form studied in [15], where Floquet theory is applied to differential-algebraic systems. To complete the bridge with the MSF, we should rewrite (13) using the direct product defined in Section II. Denoting with

$$\Delta = [\delta_1', \ldots, \delta_N']' \in \mathbb{R}^{DN},$$

we have

$$\frac{\mathrm{d}}{\mathrm{d}\,t}\Big[\Big(1_N \otimes Dq(x^T) + vZ \otimes Dr(x^T)\Big)\Delta\Big] + \Big(1_N \otimes Dg(x^T) + W \otimes Dh(x^T)\Big)\Delta = 0. \quad (14)$$

where 1_N is the identity matrix of rank N. Let $\hat{Z}$ be the matrix with $\hat{z}_1, \ldots, \hat{z}_N$, the eigenvalues of Z, on the diagonal and Q the matrix with the corresponding eigenvectors as columns. Multiplying both sides of (14) by $Q^{-1} \otimes 1_D$, we obtain

$$\frac{\mathrm{d}}{\mathrm{d}\,t}\Big[\Big(1_N \otimes Dq(x^T) + v\hat{Z} \otimes Dr(x^T)\Big)(Q^{-1} \otimes 1_D)\Delta\Big] + \\ \Big(1_N \otimes Dg(x^T) + \hat{W} \otimes Dh(x^T)\Big)(Q^{-1} \otimes 1_D)\Delta = 0. \quad (15)$$

Introducing $\Theta = (Q^{-1} \otimes 1_D)\Delta$ and $[\theta_1, \ldots, \theta_N] = \Theta$, with each $\theta_n \in \mathbb{R}^L$ and $\Theta \in \mathbb{R}^{NL}$, we can write (15) as a system composed of N uncoupled L-dimensional subsystems

$$\frac{\mathrm{d}}{\mathrm{d}\,t}[(Dq(x^T) + v\hat{z}Dr(x^T))\theta_n] + (Dg(x^T) + w\hat{z}Dh(x^T))\theta_n = 0. \quad (16)$$

The stability of the synchronous manifold is determined by the evolution of the solution θ_n of (16), as studied in Floquet theory. Let us call $\mu(v\hat{z}_n, w\hat{z}_n)$ the FE with greatest real part of (16), with $x^T(t)$ solution of (1). Since for periodic solutions LEs and the real part of FEs coincide [7], we set $\Lambda(v\hat{z}_n, w\hat{z}_n) = \mathrm{Re}(\mu(\hat{w}_n))$.

If we forget that $\hat{z}_n$ is an eigenvalue of Z and we treat it as a parameter, we could calculate the value of $\Lambda(v\hat{z}, w\hat{z})$ for $v\hat{z}, w\hat{z}$ in certain subsets of $\mathbb{C}$, resorting to numerical techniques. Thus, given the topology described by matrix Z with spectrum $0 = \hat{z}_1, \ldots, \hat{z}_N$, and given coupling strenghts v and w, we have that if $\Lambda(v\hat{z}_n, w\hat{z}_n) > 0$ for at least one $n \in \{2, \ldots, N\}$, then the synchronous state is an unstable configuration for that coupling. The value $\Lambda(v\hat{z}_1, w\hat{z}_1) = \Lambda(0, 0) = 0$. It refers indeed to the uncoupled oscillator, namely gives the FE with greatest real part of the cycle $x^T(t)$, and should be 0.

Considering symmetric couplings, the eigenvalues of Z are real. The evaluation of $\mu(\cdot, \cdot)$ can be restricted on real intervals, namely $\Lambda(v\hat{z}_n, w\hat{z}_n)$, $v\hat{z} \in \mathcal{I}_{\text{dynamic}} \subset \mathbb{R}$ and $w\hat{z} \in \mathcal{I}_{\text{static}} \subset \mathbb{R}$.

The MSF is often evaluated using time-domain based numerical algorithms that compute the maximum LE of (16), on the synchronous manifold [9], [11]. This approach usually requests a series of time consuming steps: (a) numerical integration of the differential equations, (b) discarding the

transient to reach the synchronous state, (c) further time to have the algorithm to estimate the Lyapunov exponents at the convergence. Focusing on periodic behavior, we can compute the MSF in a more efficient way working in the frequency domain. The periodic solution x^T is accurately identified by means of HB and then the eigenvalue problem of (8) is solved with A_M and C_M corresponding to $A(t)$ and $C(t)$, respectively, given by

$$\begin{cases} C(t) &= Dq(x^T) + v\hat{z}Dr(x^T), \\ A(t) &= -(Dg(x^T) + w\hat{z}Dr(x^T)). \end{cases} \tag{17}$$

As already mentioned in Section II, to get accurate results when looking for the FE with greatest real part, we should concentrate on the eigenvalues with smaller imaginary part, as pointed out in [14]. The main steps of the proposed approach are summarized in Algorithm 1.

Algorithm 1 Frequency-domain based MSF, for periodic oscillatory networks with static and dynamic couplings

Input: Equation $\frac{\mathrm{d}\,q(x)}{\mathrm{d}\,t} + g(x) = 0$ determining the evolution of the L-dimensional free oscillator; Jacobian matrices of the functions $Dq(\cdot)$, $Dr(\cdot)$, $Dg(\cdot)$, and $Dh(\cdot)$; sets $\mathcal{I}_{\text{static}}$ and/or $\mathcal{I}_{\text{dynamic}}$ where the MSF $\Lambda(\cdot, \cdots)$ has to be evaluated

Output: $\Lambda(v\hat{z}, w\hat{z})$ for each value $v\hat{z} \in \mathcal{I}_{\text{dynamic}}$, $w\hat{z} \in \mathcal{I}_{\text{static}}$.

1: Determine the steady state solution x^T and its Fourier coefficients X^F through the HB
2: **for** each $v\hat{z} \in \mathcal{I}_{\text{dynamic}}$ **do**
3: **for** each $w\hat{z} \in \mathcal{I}_{\text{static}}$ **do**
4: Solve (8) with A_M and C_M constructed using A and C given by $-(Dg + w\hat{z}Dh)$ and $Dq + v\hat{z}Dr$, respectively, evaluated on the limit cycle X^F; LM eigenvalues are obtained
5: Among the LM eigenvalues provided by the previous step, select the L eigenvalues with smaller imaginary part $\mu_1, \ldots, \mu_L$
6: $\Lambda(v\hat{z}, w\hat{z}) = \max\{\mathrm{Re}(\mu_1), \ldots, \mathrm{Re}(\mu_L)\}$
7: **end for**
8: **end for**

IV. Numerical results

This Section is devoted to present some numerical examples to validate the proposed technique. We divide them in three cases:

A) static couplings (Section IV-A),
B) dynamic coupling (Section IV-B),
C) mixed static and dynamic couplings (Section IV-C).

Case (A) is the one usually considered in literature and allows us a comparison with known results to assess the precision of the proposed method. From a circuital point of view, case (A) describes networks of oscillators coupled with linear or nonlinear resistor, whereas case (B) represents networks of oscillators coupled with linear or nonlinear capacitors, inductors, or memristors. Case (C) is more general, as both kinds of coupling elements are considered.

A. Static coupling

In order to verify the accuracy of the proposed algorithm, we study the stability of synchronous states in networks composed of Rössler's or Chua's oscillators, coupled in a static diffusive way, i.e. with $v = 0$, $w\hat{z} = \hat{w}$, and linear function $h(\cdot)$. The networks of oscillators are then described by the following differential equations

$$\dot{x}_n = f(x) - \sum_{n'=1}^{N} W_{nn'} H x_{n'}, \tag{18}$$

where $x_n = [x_{n1}, x_{n2}, x_{n3}]' \in \mathbb{R}^3$ and $H \in \mathbb{R}^{3\times 3}$. This is a well known framework, which allows us to validate the accuracy of the proposed algorithm. The matrix W describes the coupling among different cells as in (10) and the coupling function $h(x_{n'})$ is a linear function, i.e. $Hx_{n'}$. Here, we stick to the examples of [19], where the matrices H are determined by

$$H_{ij} \in \{0, 1\},\ \forall i, j \in \{1, 2, 3\},\ \text{and}\ \sum_{i,j} H_{ij} = 1. \tag{19}$$

As a consequence of (19), H has only one nonzero entry, which is equal to 1. For example, if H is everywhere 0 but for $H_{12} = 1$, then the $x_{n'2}$ component influences x_{n1}.

The MSFs for Rössler's and Chua's oscillators are derived according to Algorithm 1, without the loop starting at line 2 and setting $w\hat{z} = \hat{w}$. The results are then compared to those obtained by means of time-domain based MSFs [9], [11].

The isolated Rössler's oscillator [20], with state variable $\xi = [\xi_1, \xi_2, \xi_3]' \in \mathbb{R}^3$, is described by the following set of normalized differential equations

$$f(x) = \begin{cases} \dot{\xi}_1 = -\xi_2 - \xi_3, \\ \dot{\xi}_2 = \xi_1 + a\xi_2, \\ \dot{\xi}_3 = b + \xi_3(\xi_1 - c), \end{cases} \tag{20}$$

and we assume $a = 0.1$, $b = 0.1$, and $c = 6$. The limit cycle is approximated with $K = 35$ harmonics.

The isolated Chua's oscillator , with state variable $\xi = [\xi_1, \xi_2, \xi_3]' \in \mathbb{R}^3$, is described by the following set of normalized differential equations

$$\begin{cases} \dot{\xi}_1 = \alpha[-\xi_1 + x_2 - \eta(\xi_1)], \\ \dot{\xi}_2 = \xi_1 - \xi_2 + \xi_3, \\ \dot{\xi}_3 = -\beta\xi_2. \end{cases} \tag{21}$$

We assume $\alpha = 8, \beta = 15$, $\eta(\xi_1) = -8/7\xi_1 + 4/63{\xi_1}^3$, and we focus on one of the two asymmetric limit cycles [17], that are accurately approximated using $K = 30$ harmonics.

Figure 2 shows the MSF computed for the Rössler's oscillator in the 9 possible configurations determined by (19), using both the time-domain and the frequency-domain version. Figure 3 shows the MSF computed for the Chua's oscillator in the same configurations as above. The time-domain and the frequency-domain versions almost coincide and discrepancies, which are indeed present, do not alter the qualitative behavior, which is determined by the sign of the MSF. In particular, changes of sign of the MSF occur for similar values of the coupling parameter $\hat{w}$. On the other hand, while giving results as accurate as the time-domain based MSF, the frequency-domain MSF proposed in Algorithm 1 can be evaluated in a much shorter time: in the considered examples, the reduction in CPU time is about 90% compared to standard time-domain techniques [9], [10] not explicitly tailored for periodic attractors. The comparison is based on several numerical simulations run on the same standard desktop under MatLab. In each considered case, the MSFs are evaluated for the same number of points on the x-axis; the number of harmonics for the frequency version is chosen in order to have a distortion index [21] lower than 10^{-3} and 10^{-1} for the Chua's and Rössler's oscillator, respectively. Convergence parameters for the time-domain version are chosen looking for the minimum time to allow the algorithm to converge, on a trial and error basis. We remark that the Rössler's oscillator is more critical and a low distortion index is not achieved neither with more than 35 harmonics. However, even in this case, the qualitative behavior of the MSF is correctly reconstructed, albeit greater discrepancies are present between the time-domain and the frequency-domain versions. A mixed time-frequency approach, based on the algorithm described in [22] and applied as in [17], could lead to performances more similar to those of our algorithm, being able to exploit the periodicity of attractors as well. As a substantial difference, our version avoids to come back from the frequency domain to the time domain (gaining in robustness and in computational time) and allows an easy treatment of systems described by DAEs).

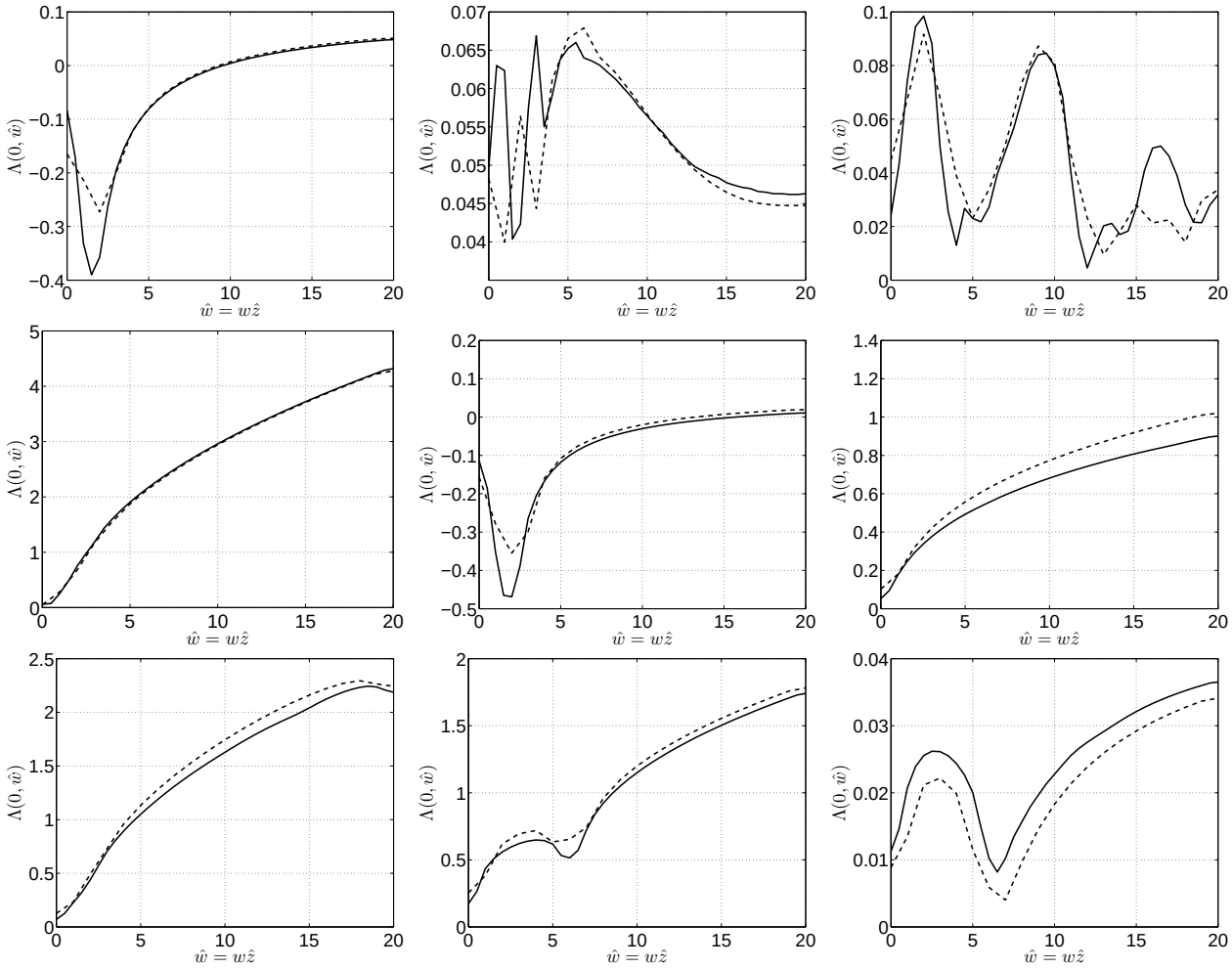

Figure 2. MSF for Rössler's oscillator with static coupling, with the 9 different configurations defined by (19). Panel i, j, in the row i from the top and column j from the left, refers to the case of component j influencing the component i, so that, for example, the panel $(1, 2)$ refers to $x_{n'2}$ influencing x_{n1}. Time domain version in solid line, frequency version in dashed line.

B. Dynamic coupling

As a further advantage, Algorithm 1 allows one to investigate synchronization in oscillatory networks with dynamic coupling ($w = 0$, $v\hat{z} = \hat{v}$). In Figure 4 we study the MSF for the Chua's oscillator with a dynamic coupling given by $r(x) = Hx$, with the same H determined by (19). We use Algorithm 1 without the loop starting at line 3 and setting $v\hat{z} = \hat{v}$. This example has never been shown in literature, to the best of our knowledge, and the results are validated with time-domain based simulations.

As a figure of merit of synchronization, we choose the mean square error among the oscillators, defined as

$$\langle e(t) \rangle = \frac{1}{\tau} \int_{t_0}^{t_0+\tau} e(t) \, \mathrm{d}\, t \tag{22}$$

where t_0 is a time instant such that the transient has vanished, τ is a sufficiently long time interval (values in the simulations are $t_0 = 1000$ and $\tau = 1000$), and

$$e(t) = \mathrm{std}(X_1(t))^2 + \mathrm{std}(X_2(t))^2 + \mathrm{std}(X_3(t))^2, \tag{23}$$

with

$$X_1(t) = \begin{bmatrix} x_{11}(t) \\ \vdots \\ x_{N1}(t) \end{bmatrix}, \; X_2(t) = \begin{bmatrix} x_{12}(t) \\ \vdots \\ x_{N2}(t) \end{bmatrix}, \; X_3(t) = \begin{bmatrix} x_{13}(t) \\ \vdots \\ x_{N3}(t) \end{bmatrix}, \tag{24}$$

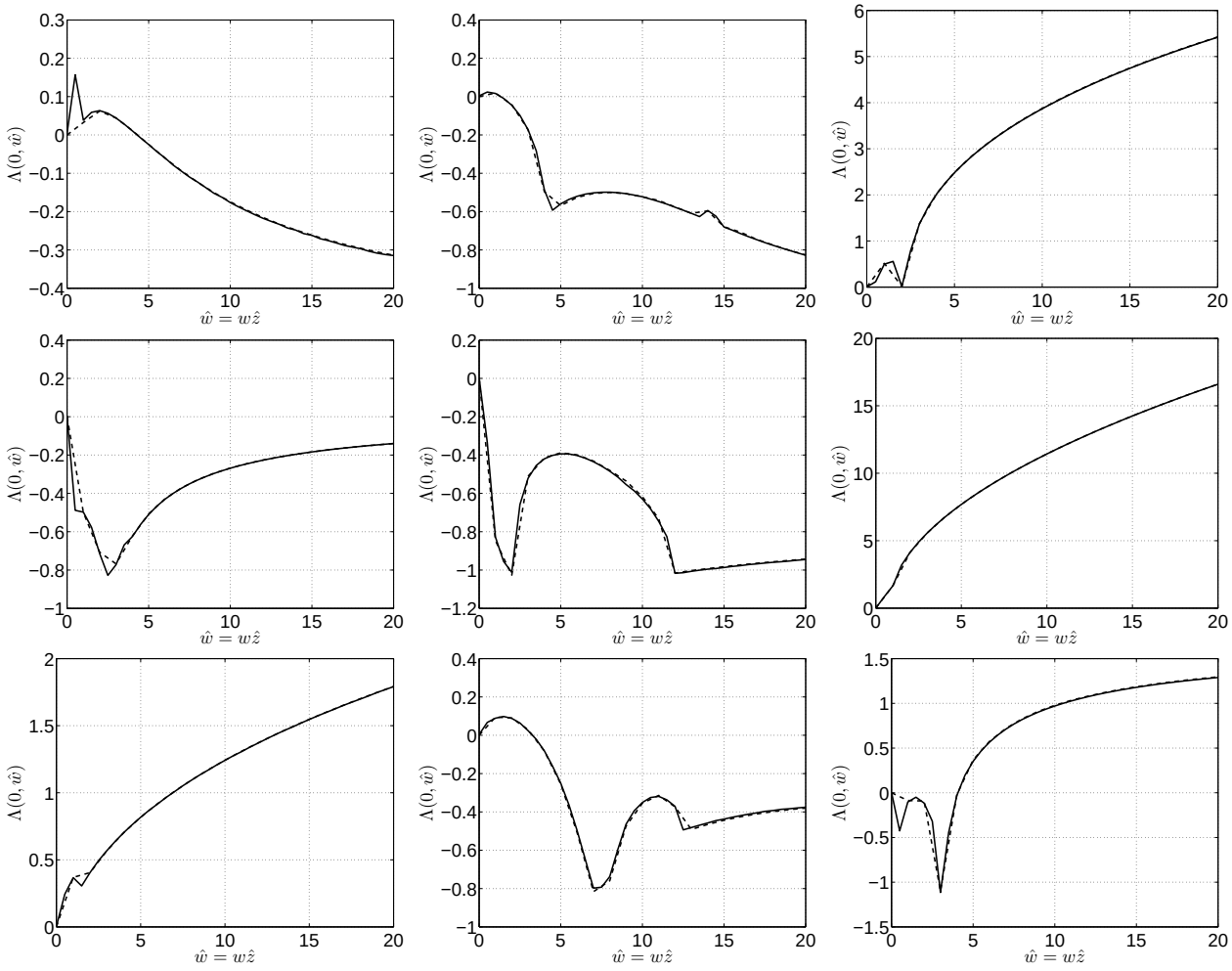

Figure 3. Msf for Chua's oscillator with static coupling, with the 9 different configurations defined by (19). Panel i, j, in the row i from the top and column j from the left, refers to the case of component j influencing the component i, so that, for example, the panel $(1, 2)$ refers to $x_{n'2}$ influencing x_{n1}. Time domain version in solid line, frequency version in dashed line.

and std$(\cdot)$ is the standard deviation. Hence, the lower is the mean square error, the better is the synchronization achieved by the network.

We focus on the two most interesting behaviors: second state variable influencing the first one and first state variable influencing the second one, corresponding to panel $(1, 2)$ and $(2, 1)$ in Figure 4, respectively.

Two kinds of networks are used in our simulations, to highlight the contribution of the overall coupling strength and the topology, two aspects which are jointly captured with the MSF approach:

- Fully connected networks,
- Ring networks.

Fully connected networks— We consider a fully connected network of 11 identical Chua's oscillators, so that $\hat{v} \in \{0, 11v\}$, where v is the global coupling strength and the matrix describing the coupling has only 2 distinct eigenvalues: 0 (with multiplicity 1) and 11 (with multiplicity 10).

When looking at the second state variable influencing the first state variable, from the MSF shape of panel $(1, 2)$ in Figure 4, we expect to have synchronization when $11v \lesssim 2.5$ or $11v \gtrsim 17$, namely $v \lesssim 0.227$ or $v \gtrsim 1.546$.

When looking at the first state variable influencing the second state variable, from the MSF shape of panel $(2, 1)$ in Figure 4, we expect to have synchronization when $11v \gtrsim 2$, namely $v \gtrsim 0.18$.

We compute $\langle e \rangle$ varying the value of v in $[0, 2]$, to verify that the predicted threshold are

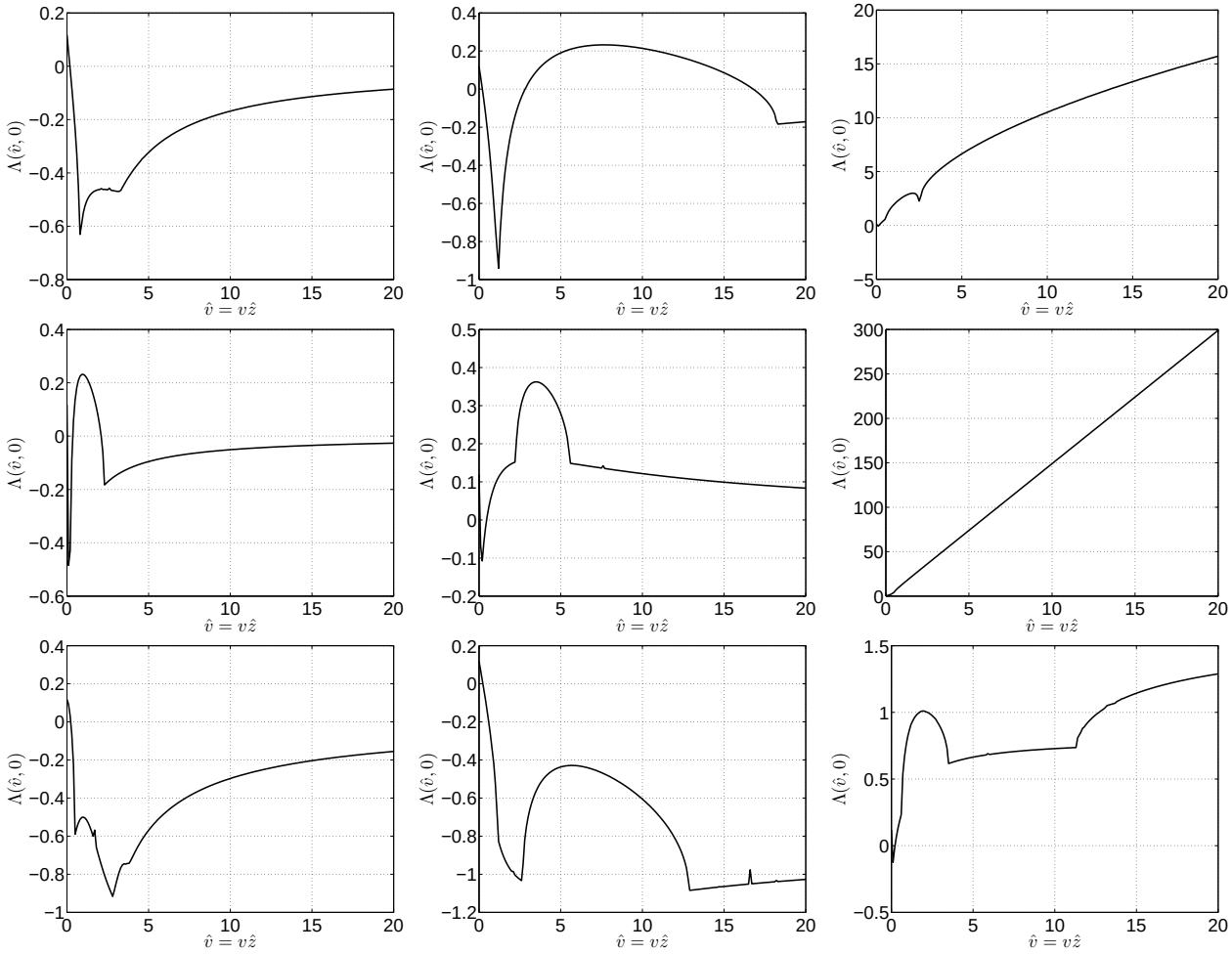

Figure 4. Msf for Chua's oscillator with dynamic coupling, with the 9 different configurations defined by (19). Panel i,j, in the row i from the top and column j from the left, refers to the case of component j influencing the component i, so that, for example, the panel $(1,2)$ refers to $x_{n'2}$ influencing x_{n1}. Only the frequency version obtained with Algorithm 1 is presented.

numerically verified in the time-domain: Figure 5 shows $\langle e\rangle$ as a function of v for the first and the second coupling configuration on the left and the right panel respectively.

Ring networks— We consider a ring of 11 identical Chua's oscillators. The spectrum of matrix V describing this coupling is given by 0, $0.318v$, $\ldots$, $3.919v$.

When examining the second state variable influencing the first one, from the MSF shape of panel $(1,2)$, Figure 4, we expect to have synchronization when $3.919v \lesssim 2.5$ or when $0.318v \gtrsim 17$, namely when $v \lesssim 0.638$ or $v \gtrsim 53.459$.

When examining the first state variable influencing the second one, from the MSF shape of panel $(2,1)$ in Figure 4, we expect to have synchronization when $0.317v \gtrsim 2$ namely $v \gtrsim 6.309$.

We compute $\langle e\rangle$ varying the value of v in $[0,60]$, for the configuration $(1,2)$ and varying $v \in [0,10]$ for the configuration $(2,1)$, to verify that the predicted thresholds are numerically verified in the time-domain: Figure 6 shows $\langle e\rangle$ as a function of v for the first and the second coupling configuration on the left and the right panel respectively.

C. Static and dynamic coupling

As a final case, we consider both dynamic and static couplings, so that the MSF is really a function of both $v\hat{z}$ and $w\hat{z}$. The results are given in Figure 7, setting $r(x) = Hx$ and $h(g) = Hx$, for the possible configurations determined by (19). The value of $v\hat{z}$ are on the x-axis, the values of

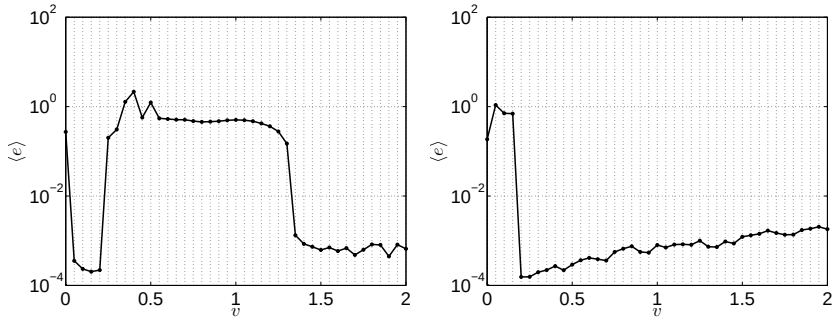

Figure 5. Mean square error, in a fully connected network of Chua's oscillators with dynamic couplings, as a function of the coupling strength. The left panel refers to the second state variable influencing the first, first state variable influencing the second one on the right panel.

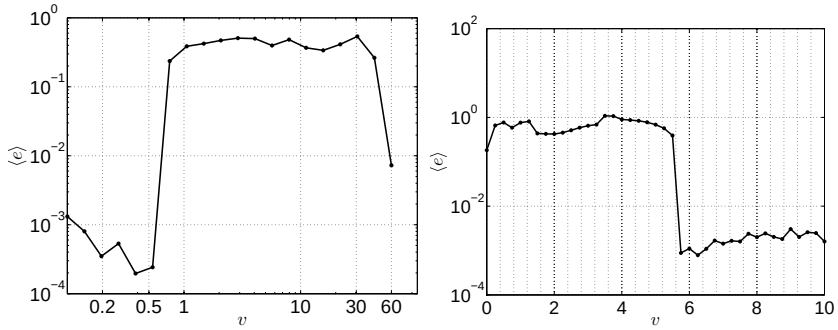

Figure 6. Mean square error, in ring connected network of Chua's oscillators with dynamic coupling, as a function of the coupling strength. The left panel refers to the second state variable influencing the first, first state variable influencing the second one on the right panel.

$w\hat{z}$ are on the y-axis, and the shade of gray codifies the value of $\Lambda(v\hat{z},\, w\hat{z})$: white correspond to $\Lambda(v\hat{z},\, w\hat{z}) < 0$, gray to $\Lambda(v\hat{z},\, w\hat{z}) > 0$.

These results, which are new in literature, are again validated through numerical simulations. We focus on fully connected networks of 11 Chua's oscillators, so that $\hat{z} \in \{0, 11\}$, and consider three cases among the possible configurations to test:

- second state variable influencing the first state variable, Figure 4, panel $(1, 2)$;
- second state variable influencing the second one, Figure 4, panel $(2, 2)$;
- third state variable influencing the third one, Figure 4, panel $(3, 3)$.

Case $(1, 2)$— We fix $w = 4/11 \approx 0.364$ and we let v vary in $[0, 20/11] \approx [0, 1.818]$, so that $w\hat{z} \in \{0, 4\}$ and $v\hat{z} \in [0, 20]$. This corresponds to moving along the dashed vertical line of panel $(1, 2)$ of Figure 7. We should have synchronization when $v\hat{z} \in (0, 6/11)$, approximatively, or $v\hat{z} \gtrsim 14$, which means $v \in (0, 6/11) \approx (0, 0.546)$ or $v \gtrsim 14/11 \approx 1.273$, as confirmed in Figure 8, left panel.

Case $(2, 2)$— We let v and w vary in $[0, 10/11] \approx [0, 0.909]$, so that $w\hat{z} \in [0, 10]$ and $v\hat{z} \in [0, 10]$. This corresponds to moving along the dashed line of panel $(2, 2)$ of Figure 7. We should have synchronization when $v\hat{z} \in (0.3, 1.7)$, approximatively, or $v\hat{z} \gtrsim 4.5$, i.e. $v \in (0.3/11, 1.7/11) \approx (0.027, 0.155)$ or $v \gtrsim 4.5/11 \approx 0.409$, as confirmed in Figure 8, central panel.

Case $(3, 3)$— We fix $v = 1/11 \approx 0.091$ and we let w vary in $[0, 7/11] \approx [0, 0.636]$, so that $v\hat{z} \in 0, 1$ and $w\hat{z} \in [0, 7]$, which corresponds to moving along the dashed horizontal line of panel $(3, 3)$ of Figure 7. We should have synchronization when $v\hat{z} \in (3.5, 4.7)$, approximatively, i.e. $v \in (3.5/11, 4.7/11) \approx (0.318, 0.427)$, as confirmed again in Figure 8, right panel.

V. Conclusion

We have proposed an efficient and accurate method to study condition for stable local synchronization in networks of identical nonlinear periodic oscillators exploiting the MSF approach in the

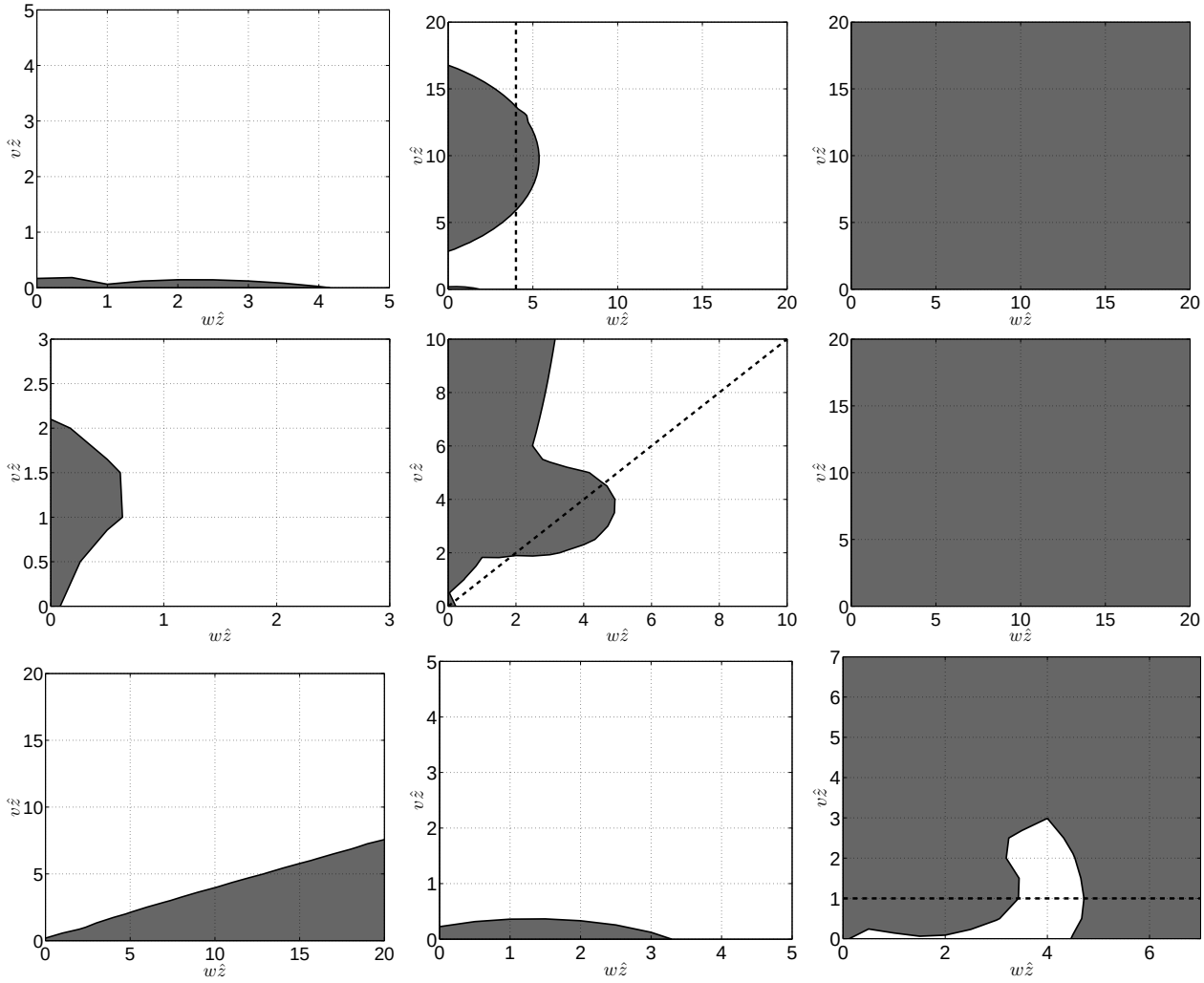

Figure 7. MSF for Chua's oscillator with static and dynamic coupling, with the 9 different configurations defined by (19). Panel i, j, in the row i from the top and column j from the left, refers to the case of component j influencing the component i, so that, for example, the panel $(1, 2)$ refers to $x_{2n'}$ influencing x_{1n}.

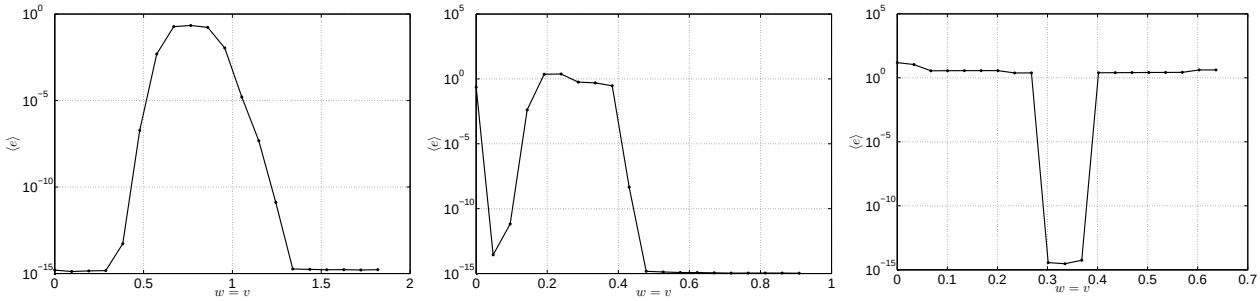

Figure 8. Mean square error for a fully connected network of 11 Chua's oscillators coupled both on the derivative and the right-hand side. The left panel refers to the case $(1, 2)$, the central panel refers to the case $(2, 2)$, and the case $(3, 3)$ is considered in the right panel.

frequency domain. Once limit cycles of uncoupled oscillators are approximated using a HB technique, an eigenvalue problem is solved to study stability. The proposed method presents advantages in terms of computational time and can also deal with oscillators described by implicit differential equations. This means that both static and dynamic coupling can be studied.

VI. Acknowledgements

This work was partially supported by the CRT Foundation, under projects no. 2009.0570 and 2010.1643, by the Istituto Superiore Mario Boella and the regional government of Piedmont.

References

[1] M. R. Arkady Pikovsky and J. Kurths, *Synchronization: A Universal Concept in Nonlinear Science*. Cambridge University Press, 2002.

[2] X. Wu, J. Cai, and Y. Zhao, "Some new algebraic criteria for chaos synchronization of Chua's circuits by linear state error feedback control," *International Journal of Circuit Theory and Applications*, vol. 34, no. 3, pp. 265–280, 2006. [Online]. Available: http://dx.doi.org/10.1002/cta.350

[3] M. Jalili, A. A. Rad, and M. Hasler, "Enhancing synchronizability of dynamical networks using the connection graph stability method," *International Journal of Circuit Theory and Applications*, vol. 35, no. 5-6, pp. 611–622, 2007. [Online]. Available: http://dx.doi.org/10.1002/cta.436

[4] E. M. Izhikevich, *Dynamical Systems in Neuroscience: The Geometry of Excitability and Bursting*. The MIT Press, Boston, MA (U.S.A), 2007.

[5] P. R. Roelfsema, A. K. Engel, P. König, and W. Singer, "Visuomotor integration is associated with zero time-lag synchronization among cortical areas," *Nature*, vol. 385, pp. 157 – 161, 1997.

[6] N. Tabareau, J.-J. Slotine, and Q.-C. Pham, "How synchronization protects from noise," *PLoS Comput Biol*, vol. 6, no. 1, p. e1000637, 01 2010. [Online]. Available: http://dx.doi.org/10.1371/journal.pcbi.1000637

[7] C. Chicone, *Ordinary Differential Equations with Applications*. Springer-Verlag New York, 1999, vol. 34.

[8] J. P. Eckmann and D. Ruelle, "Ergodic theory of strange attractors," *Rev. Mod. Phys.*, vol. 57, pp. 617–656, 1985.

[9] A. Wolf, J. B. Swift, H. L. Swinney, and J. A. Vastano, "Determining Lyapunov Exponents from a Time Series," *Physica D*, vol. 16, pp. 285 – 317, 1985.

[10] K. Geist, U. Parlitz, and W. Lauterborn, "Comparison of different methods for computing Lyapunov exponents," *Progress of Theoretical Physics*, vol. 83, no. 5, pp. 875–893, 1990.

[11] L. M. Pecora and T. L. Carroll, "Master stability functions for synchronized coupled systems," *Phys. Rev. Letters*, vol. 80, no. 10, pp. 2109– 112, Mar. 1998.

[12] A. I. Mees, *Dynamics of feedback systems*. Wiley, 1981.

[13] M. Righero, F. Corinto, and M. Biey, "An efficient algorithm for the evaluation of master stability function in networks of coupled oscillators," in *Proceedings of NOLTA 2010, Krakow*, 2010.

[14] F. L. Traversa, F. Bonani, and S. Donati Guerrieri, "A frequency-domain approach to the analysis of stability and bifurcation in nonlinear systems described by differential-algebraic equations," *Int. J. Circ. Theor. Appl.*, vol. 36, pp. 421–439, 2008.

[15] A. Demir, "Floquet theory and non-linear perturbation analysis for oscillators with differential-algebraic equations," *Internationl Journal of Circuit Theory and Applications*, vol. 28, no. 2, pp. 163–185, 2000.

[16] A. Brambilla and G. Storti Gajani, "Computation of all the Floquet eigenfunctions in autonomous circuits," *International Journal of Circuit Theory and Applications*, vol. 36, no. 5-6, pp. 717–737, 2008. [Online]. Available: http://dx.doi.org/10.1002/cta.457

[17] M. Gilli, F. Corinto, and P. Checco, "Periodic oscillations and bifurcations in cellular nonlinear networks," *IEEE Trans. Circ. Syst. I*, vol. 51, no. 5, pp. 948–962, 2004.

[18] F. Corinto, V. Lanza, and M. Gilli, "Spiral waves in bio-inspired oscillatory dissipative media," *International Journal of Circuit Theory and Application*, vol. 36, no. 5-6, pp. 555–571, 2008.

[19] Y.-C. L. Liang Huang, Qingfei Chen and L. M. Pecora, "Generic behavior of master-stability functions in coupled nonlinear dynamical systems," *Physical Review E*, vol. 80, no. 036204, 2009.

[20] O. E. Rössler, "An equation for continuous chaos," *Physics Letters A*, vol. 57, no. 5, pp. 397–398, 1976.

[21] R. Genesio, A. Tesi, and F. Villoresi, "A frequency approach for analyzing and controlling chaos in nonlinear circuits," *Circuits and Systems I: Fundamental Theory and Applications, IEEE Transactions on*, vol. 40, no. 11, pp. 819 –828, nov 1993.

[22] M. Farkas, *Periodic motions*. New York, NY, USA: Springer-Verlag New York, Inc., 1994.